Effect of initial crystallized silicon layer on the properties of microcrystalline silicon grown by internal inductively coupled plasma-type plasma enhanced chemical vapor deposition

H.C. Lee [a], H.B. Kim [b], G.Y. Yeom [a,*], I.H. Park [c], Y.W. Kim [c]

[a] Department of Advanced Materials Science & Engineering, Sungkyunkwan University, Suwon, Gyeonggi-Do, 440-746, Republic of Korea
[b] Advanced Institute of Nano Technology, Sungkyunkwan University, Suwon, Gyeonggi-Do, 440-746, Republic of Korea
[c] Department of Materials Engineering, Seoul National University, Seoul, 151-742, Republic of Korea

ARTICLE INFO

ABSTRACT

Using an internal inductively coupled plasma (ICP)-type-plasma enhanced vapor deposition system, microcrystalline silicon thin films were deposited as a function of H_2/SiH_4 gas ratio at 180 °C. Especially, the effects of deposition with/without an initial thin silicon layer formed with a very high hydrogen percentage on the microstructure of the deposited silicon thin film were investigated. The deposited silicon thin film showed higher crystallization percentage at the higher hydrogen percentage in H_2/SiH_4 due to the high ratio of H/SiH in the plasma. At the same gas mixture of H_2/SiH_4, the deposition of silicon thin film after the formation of an initial silicon layer with a high hydrogen percentage on the glass substrate increased the crystallization percentage from 3 to 14%. The initial silicon layer deposited with a high hydrogen percentage showed a nanocrystalline grain structure; therefore, the nanocrystalline structure in the initial silicon layer appeared to act as a nucleation site for the growth of microcrystalline silicon thin films. Using the internal ICP-PECVD, the microcrystalline silicon having about 87% of crystallization could be deposited on the glass substrate at 180 °C with the 90% of hydrogen dilution percentage and with the thin initial silicon layer.

© 2008 Elsevier B.V. All rights reserved.

1. Introduction

Considerable attention has been paid to hydrogenated microcrystalline or nano-crystalline silicon film deposited at low temperature because of its promising application to stable high efficient solar cell, thin film transistors, color sensors, etc. [1,2]. In particular, the development of microcrystalline silicon film is one of the key issues in developing active matrix liquid crystal displays (AMLCD) and active matrix organic light emitting displays (AMOLED). However, during the initial stage of the hydrogenated microcrystalline silicon film growth process, amorphous silicon layer is generally formed before the nucleation and growth of the microcrystalline silicon on the glass substrate [3]. This amorphous silicon initial layer affects the electrical characteristics of the grown thin film such as carrier transport along the film growth direction and deteriorates the device performance [4].

For the flat panel display (FPD) device processing, capacitively coupled plasma (CCP) sources are generally employed due to the excellent plasma uniformity over the large area substrate even though the processing throughput is low due to the low plasma density of the CCP source. However, to improve device processing properties such as the increase of the throughput, the decrease of the processing

temperature, etc., various high-density plasma sources have been recently studied for the material processing of thin film transistor-liquid crystal display (TFT-LCD) by using various tools such as an array of helicon source [5], an external inductively coupled plasma (ICP) source composed of a large loop antenna [6], ICP sources composed of internal linear antennas [7,8], etc. Among these sources, internal-type ICP sources which do not require a thick dielectric window for transmitting the electromagnetic field to the plasma from the source antennas and which are easily extendable to large area have been intensively studied for the application to next generation FPD materials processing.

In this study, silicon thin film was deposited at a low temperature of 180 °C by using an internal ICP-plasma enhanced chemical vapor deposition (PECVD) in H_2/SiH_4, and the effect of hydrogen percentage in H_2/SiH_4 on the degree of crystallization of the silicon thin film was investigated. Especially, the effect of an initial thin crystallized silicon layer before the deposition of silicon thin film on the final crystal structure of the grown silicon thin film was investigated.

2. Experimental

A schematic diagram of the internal-type ICP-PECVD system used in the experiment is shown in Fig. 1. The processing chamber was a rectangular shape and the inner size of the chamber was 1020 mm × 830 mm and the substrate size was 470 mm × 370 mm. The samples were loaded to

* Corresponding author. Tel.: +82 31 299 6562; fax: +82 31 299 6565.
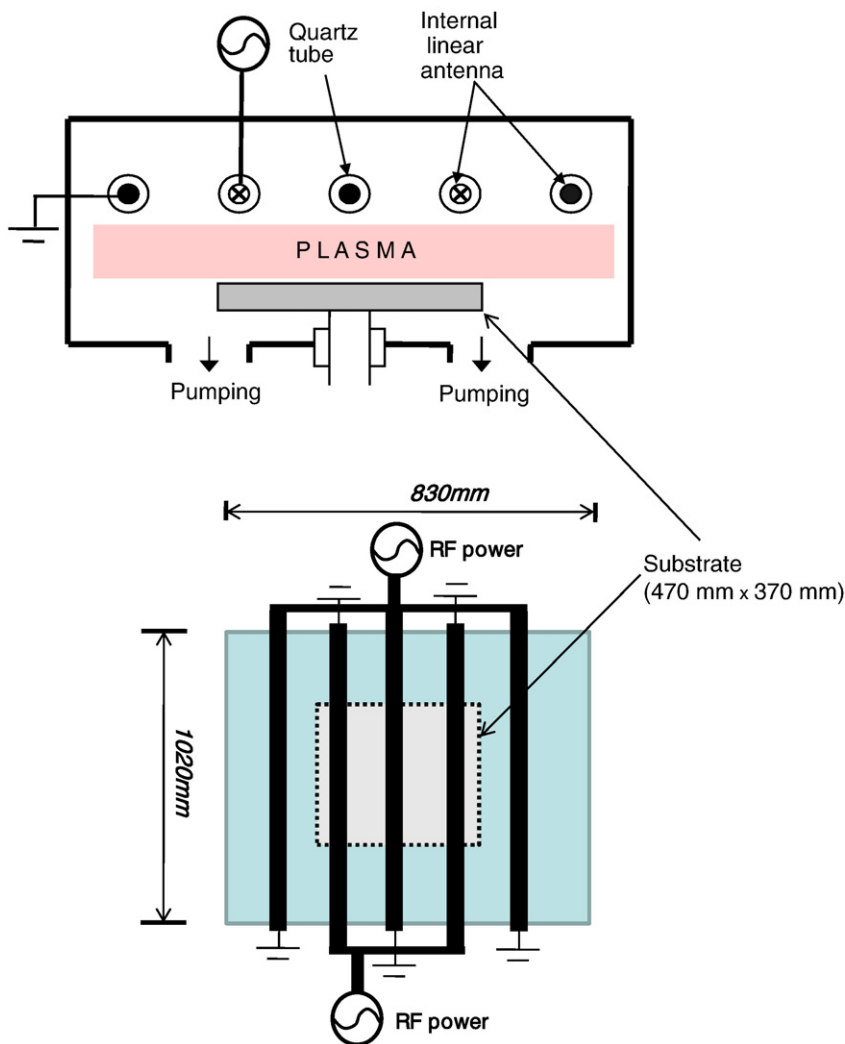E-mail address: gyyeom@skku.edu (G.Y. Yeom).

Fig. 1. Schematic diagram of the internal ICP-PECVD system used in this experiment for the deposition of microcrystalline silicon thin film.

the substrate holder in vacuum through a loadlock chamber. The antenna for the internal-type ICP was made of 10 mm diameter copper tubing covered with quartz tubing of 15 mm in diameter and 2 mm in thickness. Five linear antennas were embedded in the process chamber, and each antenna was connected to an RF power supply (13.56 MHz) through a matching network alternatively from the opposite ends to form a "double comb-type antenna". The other end of the antennas was grounded. More details of the system can be found elsewhere [9,10].

Corning 1737 glass was used as the substrate and, to deposit microcrystalline silicon thin films on the glass substrates, gas mixtures composed of SiH_4 and H_2 were used and the ratio of $H_2/[H_2+SiH_4]$ (R= $[H_2/[H_2+SiH_4]]*100$) was varied from 10 to 95% while keeping the total gas flow rate at 200 sccm. During the deposition of the silicon thin films, the rf power density was maintained at 0.48 W/cm^2 by applying 4 kW of rf power to the ICP source, the processing chamber pressure was maintained at 20 mTorr, and the substrate temperature was maintained at 180 °C (the substrate temperature was measured on the substrate surface using a thermocouple). Especially, to study the effect of an initial thin crystallized silicon layer on the final structure of the silicon thin, about 30 nm thick silicon layer was initially deposited on the glass substrate before the deposition of main silicon layer. The initial 30 nm thick silicon layer was deposited with a gas mixture condition of the high hydrogen percentages (deposited with R=95% for 100 s followed by deposition with R=93% for 60 s), while the following main silicon layer was deposited with different hydrogen dilution percentages.

The degree of the crystallinity of the deposited thin films was investigated using Raman spectroscopy (Kaiser, Rxn1) and the surface roughness was measured by atomic force microscopy (AFM, Thero-microscopy, CP Research). The structure of the deposited film was investigated by a high resolution X-ray diffraction method (HRXRD, D8 Discover Bruker) using Cu Kα$_1$ (1.54 Å). Using high resolution transmission electron microscopy (HRTEM, JEOL JEM 3000F), the detailed microstructures of the deposited thin film such as interface structure, the grain size, etc. were observed. The change of radical species in the plasma during the deposition by H_2/SiH_4 as a function of hydrogen dilution percentage was investigated by optical emission spectroscopy (OES, PCM 420 SC Technology).

3. Results and discussion

Fig. 2 shows the optical emission peaks of H_α^* (observed at 656 nm) and SiH* (observed at 413 nm) and the ratio of H_α^*/SiH* measured using OES as a function of hydrogen dilution percentage R (R=$[H_2/[H_2+SiH_4]]*100$) from 10 to 95%. The rf power density, the operating pressure, and the total gas flow rate were maintained at 0.48 W/cm^2, 20 mTorr, and 200 sccm, respectively. As shown in the figure, when the hydrogen percentage in the gas mixture was increased, the optical emission peak intensity of H_α^* in the plasma was increased while the peak intensity of SiH* was decreased. Especially, when the R was higher than 90%, significant increase of H_α^* and significant decrease of SiH* could be observed. Therefore,
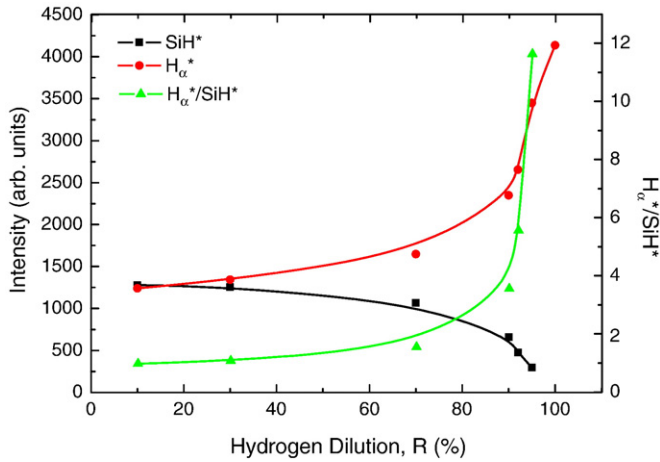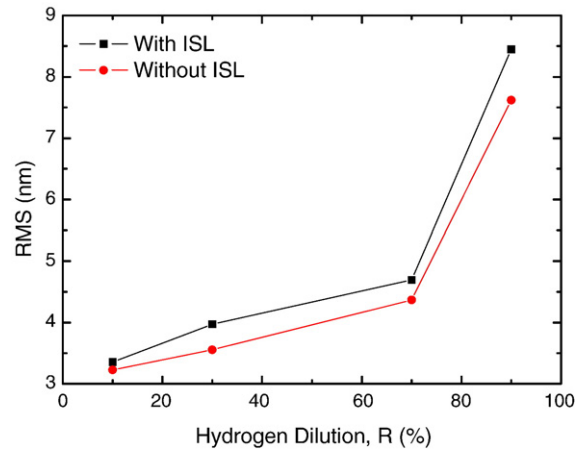
Fig. 2. OES peak intensities of H_α^* and SiH* in H_2/SiH$_4$ and the ratio of H_α^*/SiH* as a function of hydrogen dilution percentage. The rf power density, the operating pressure, and the total gas flow rate were maintained at 0.48 W/cm^2, 20 mTorr, and 200 sccm, respectively.

the increase of hydrogen percentage, R, initially increased the ratio of H_α^*/SiH* slowly and, when the R is higher than 90%, the ratio of H_α^*/SiH* increased significantly. H_α^* in the plasma originates from the decomposition of H_2 and SiH$_4$ and, it is known that, the increase of the ratio of H_α^*/SiH* increases the crystallization of the deposition silicon thin film [11,12].

To observe the differences of the silicon thin film structure between the silicon film deposited with a high R and that with a low R, about 30 nm thick initial silicon layers were deposited on glass substrates (RMS surface roughness of glass substrate: 0.495 Å) and the surface roughness measured by AFM was compared (not shown). The RMS surface roughness of a 30 nm-thick initial silicon layer deposited on a glass substrate with a high R (the initial silicon layer (ISL) deposited with R=95% for 100 s followed by deposition with R=93% for 60 s) was about 4.78 Å and the surface roughness of an initial silicon layer deposited with R=0% for 40 s was about 3.85 Å. Therefore, higher surface roughness was obtained with the initial silicon layer deposited with the high R. The increased RMS surface roughness obtained with the high R is believed to be from the high crystallization percentage of the deposited silicon layer [13] due to the high ratio of H_α^*/SiH* in the plasma.
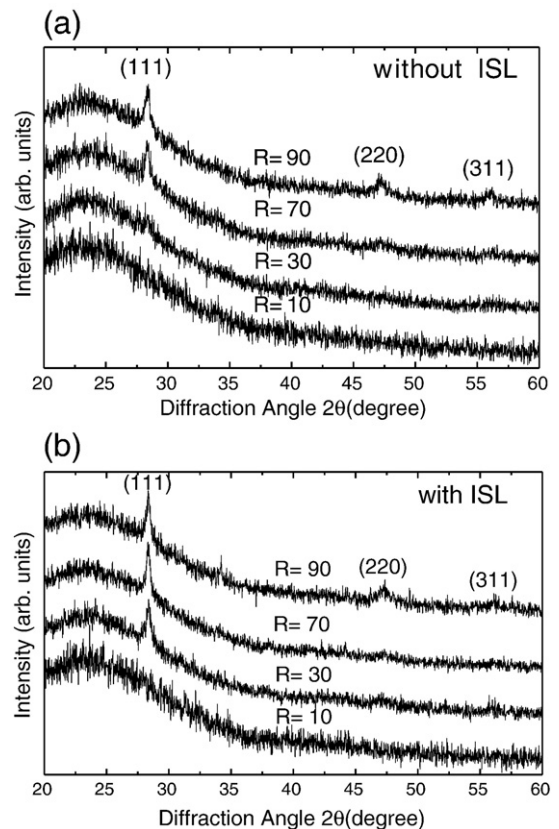
The initial crystallized silicon layer deposited on the glass substrate may act as a nucleation site and seed for the growth of microcrystalline silicon. Therefore, about 450 nm-thick silicon thin films was deposited as a function of hydrogen percentage on the glass substrate with/without the 30 nm-thick initial thin silicon layer, and the effect of the initial silicon layer on the structure of the final silicon thin film deposited with different hydrogen percentages was investigated. Fig. 3 shows the RMS surface roughness of silicon thin films deposited on the glass substrate with/without the initial crystallized silicon layer as a function of the hydrogen dilution percentage. The plasma condition was the same as the condition in Fig. 2 while the deposition temperature was maintained at 180 °C. As shown in the figure, the increase of R in the gas mixture increased the RMS surface roughness for both films deposited on the glass substrate with and without the initial silicon layer possibly due to the increase of the crystallization percentage in the deposited thin film. However, the silicon thin films deposited with the initial silicon layer showed higher surface roughness compared to those deposited without the initial silicon layer possibly due to the higher crystallization percentage of the grown silicon thin film at the same hydrogen percentage in the gas mixture.

The crystal structure of the silicon thin films deposited with and without the initial silicon layer as a function of R from 10 to 90% was

investigated by HRXRD and the results are shown in Fig. 4(a) for the silicon films with the initial silicon layer and (b) for the silicon films without the initial silicon layer. As shown in the figure, the silicon thin films deposited with higher hydrogen dilution ratio showed sharper diffraction peaks related to (111), (220), and (311) crystallographic planes for both thin films deposited with and without the initial silicon layer showing higher crystallization of the thin film deposited with higher R. Also, as shown in the figure, the XRD of the thin film deposited with the initial silicon layer showed higher peak intensities related to the crystallographic planes at the same R indicating the

Fig. 3. AFM surface roughness of silicon thin film deposited as a function of hydrogen percentage in H_2/SiH$_4$ on the glass substrate with/without an initial highly crystallized silicon layer (ISL). The substrate temperature was maintained at 180 °C. 30 nm-thick thick ISL was deposited on the glass substrate with R=95% for 100 s followed by deposition with R=93% for 60 s.

Fig. 4. XRD data of the microcrystalline silicon thin films deposited as a function of hydrogen percentage (a) without the ISL and (b) with the ISL.

higher crystallization percentage for the thin film deposited with the initial silicon layer.

The degree of crystallization of the silicon thin films grown with and without the initial silicon layer was quantitatively investigated as a function of R using Raman spectroscopy and the results are shown in Fig. 5. The Raman spectra could be deconvoluted into three peaks located at 480 cm^{-1} originated from amorphous silicon, and 510 and 520 cm^{-1} originated from crystalline silicon. As shown in the figure, similar to the results obtained by the AFM data in Fig. 3 and the XRD data in Fig. 4, the increase of R increased the peak intensities related to the crystalline peaks indicating the increase of crystallization with the increase of R. Also, the silicon thin film deposited with the initial silicon layer showed higher Raman peaks related to the crystalline silicon at the same R. The crystalline volume fraction (X_c) was calculated by $X_c = A_{510} + A_{520} / A_{480} + A_{520} + A_{510}$, [14] and the crystalline volume fraction of the silicon thin films calculated from the Raman spectra in Fig. 5 is shown in Fig. 6 as a function of R and with/without the initial silicon layer. The increased crystallization percentage with the initial silicon layer is also shown in the figure. As shown in the figure, the increase of R from 10 to 90% increased the crystallization percentage of the silicon thin film grown without the initial silicon layer significantly from about 8% to 84%. However, when the silicon thin film was grown on the thin initial silicon layer, as shown in the figure, the further increase of crystallization percentage from 14 (at R=10%) to 3% (at R=90%) could be obtained. Therefore, it is believed that the formation of an initial thin silicon layer with a highly crystallization percentage before the deposition of main silicon thin film increases the crystallization of the following silicon thin film by acting as nucleation site or seed for crystallization. Even though the higher crystallization percentage can be obtained by depositing with a higher hydrogen dilution percentage, the increased hydrogen dilution in the gas mixture generally decreases the deposition rate, therefore, the use of the initial silicon layer can
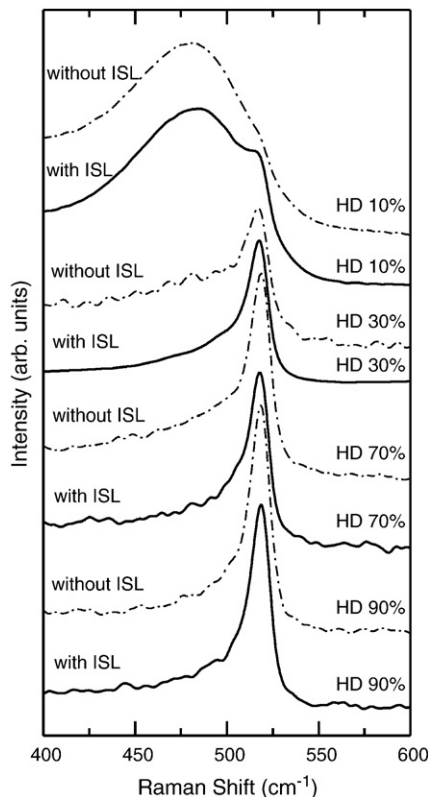

Fig. 6. Crystalline volume faction of the silicon thin film deposited as a function of hydrogen percentage on the glass substrate with/without the initial silicon layer.

improve the deposition rate without decreasing the crystallization percentage of the grown silicon thin film.

The microstructure of the silicon thin film grown with the initial silicon layer at the hydrogen percentage of 90% was observed using the TEM. Fig. 7(a) shows the cross-sectional TEM of silicon thin film deposited with the initial silicon layer and (b) shows the HRTEM of the interface between the SiO$_2$ and the initial silicon layer. As shown in HRTEM of Fig. 7(b), the initial silicon layer was composed of nanocrystalline silicon grains having about 10 nm diameter grain size. Also, as shown in Fig. 7(a), long microcrystalline silicon grains were observed in a direction normal to the substrate. The diffraction pattern shown in the inset of Fig. 4(a) also shows the high crystallinity of the deposited silicon thin film. Therefore, the initial crystallized

Fig. 5. Raman spectra of the microcrystalline silicon thin films deposited as a function of hydrogen percentage on the glass substrate with/without the initial silicon layer.
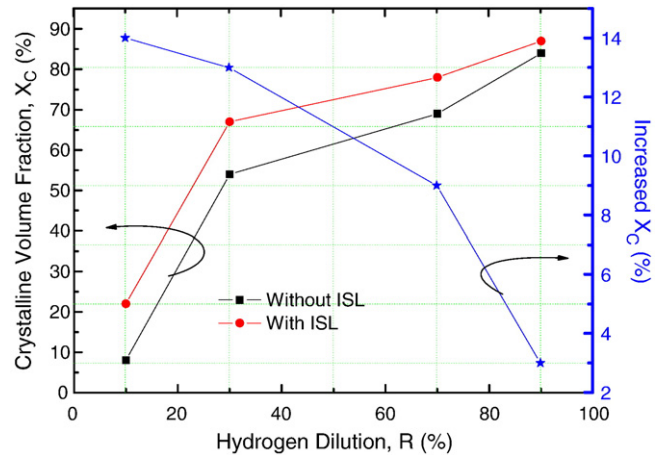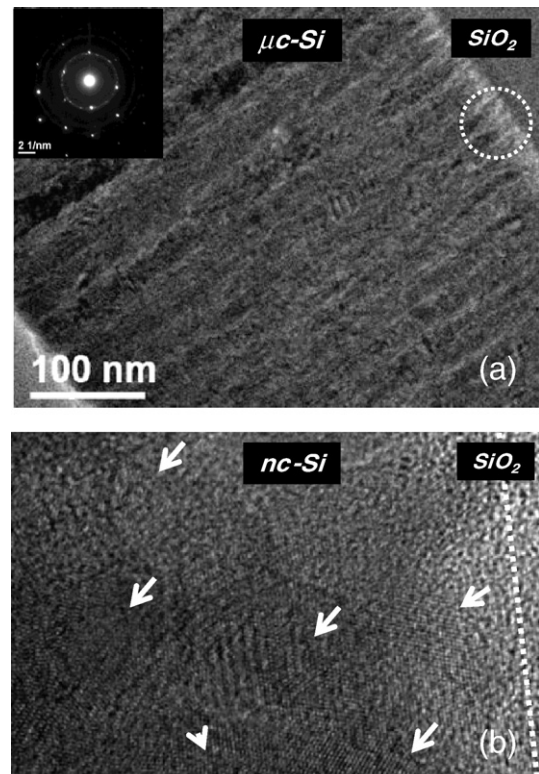

Fig. 7. (a) Cross-sectional TEM of silicon thin film grown with the initial silicon layer and (b) the HRTEM of the interface between the SiO$_2$ and the initial silicon layer. The hydrogen dilution percentage during the deposition of silicon thin film was 90%.

silicon layer appeared to assist in increasing the crystallization of the growing silicon thin film by acting as the nucleation site for microcrystalline grains.

4. Conclusions

Using an internal-type ICP-PECVD, microcrystalline silicon thin films were deposited at 180 °C as a function of gas mixture ratio of H_2/SiH_4 with/without an initial thin silicon layer formed with a very high hydrogen percentage and the effect of hydrogen dilution percentage and the initial silicon layer on the microstructure of the grown silicon thin film was investigated.

The deposition of silicon thin film at the higher hydrogen dilution percentage showed higher RMS surface roughness, higher XRD peaks related to the crystallographic planes such as (111), (220), etc., and the higher Raman peaks related to the crystalline silicon indicating higher crystallization percentage of the silicon thin film deposited with higher hydrogen dilution percentage. Also, the formation of a 30 nm-thick silicon layer with a very high hydrogen dilution percentage on the glass substrate before the deposition of the silicon thin film with various hydrogen dilution percentage increased the crystallization further at the same hydrogen dilution percentage. The increase of crystallization percentage with the increase of hydrogen dilution percentage was believed to be related to the increase of H_{α}^*/SiH^* in the plasma. The higher crystallization of the silicon thin film deposited with the initial silicon layer was believed to be related to the formation of nucleation site or seed for the microcrystalline silicon by the nanocrystalline silicon in the initial silicon layer as observed by the HRTEM.

Acknowledgment

References

[1] B. Rech, T. Roschek, T. Repmann, J. Muller, R. Schmitz, W. Appenzeller, Thin Solid Films 427 (2003) 157.
[2] J.P. Kleider, C. Longeaud, R. Bruggemann, F. Houze, Thin Solid Films 383 (2001) 57.
[3] F.F. Chen, X.C. Jiang, J.D. Evans, J. Vac. Sci. Tech. A 18 (2000) 2108.
[4] Y. Setsuhara, S. Miyake, Y. Sakawa, T. Shoji, Jpn. J.Appl. Phys. 38 (1999) 4263.
[5] Y. Wu, M.A. Lieberman, Appl. Phys. Lett. 72 (1998) 777.
[6] K.N. Kim, Y.J. Lee, S.J. Kyong, G.Y. Yeom, Surf. Coat. Technol. 752 (2004) 177.
[7] Toshihiko Toyama, Hiroaki Okamoto, Sol. Energy 80 (2006) 658.
[8] P. Roca i Cabarrocas, J. Non-cryst. Solids 31 (2000) 266.
[9] S.J. Jung, K.N. Kim, G.Y. Yeom, Thin Solid Films 506 (2006) 460.
[10] K.N. Kim, M.S. Kim, G.Y. Yeom, Appl. Phys. Lett. 88 (2006) 161503.
[11] A. Matsuda, J. Non-Cryst. Solids 338 (2004) 1.
[12] S. Sriraman, S. Agarwal, E.S. Aydil, D. Maroudas, Nature 418 (2002) 62.
[13] J.H. Zhou, K. Ikuta, T. Yasuda, T. Umeda, S. Yamasaki, K. Tanaka, J. Non-cryst. Solids 227 (1998) 857.
[14] S. Furukawa, T. Miyasato, Phys. Rev. B 38 (1988) 5726.